Azimuthally Invariant Mueller-Matrix Tomography of Linear Dichroism of Polycrystalline Networks of Biological Tissues

A.Pavlyukovich[1)], N. Pavlyukovich[1)],Y.Sarkisova[1)], A. Dubolazov[2)], O.Ushenko[2)], V. Ushenko[2)], M.Kovalchuk[2)], Yu. Solovey[1)], M. Solovey[1)], S. Railianu[1)], V. Polovyi[1)]

[1)] *Bukovinian State Medical University, 3 Theatral Sq., Chernivtsi, Ukraine, 58000*
[2)] *Chernivtsi National University, 2 Kotsiubynskyi Str., Chernivtsi, Ukraine, 58012*
a.dubolazov@chnu.edu.ua

ABSTRACT

The results of applying algorithms for reconstructing parameters characterizing the linear dichroism of networks of biological crystals in differentiating changes in optical anisotropy associated with varying degrees of severity of pathology — pre-cancerous (atrophy and endometrial polyp) states of the cervix are presented.

Keywords: Mueller matrix tomography, linear dichroism, biological tissue, diagnostic.

1. Introduction

To analyze the manifestations of amplitude anisotropy, we used the short-wavelength region of the spectrum (λ_2), where the maxima of the optically anisotropic absorption of protein molecules are localized. The information on amplitude anisotropy is contained in the values of three azimuthally independent matrix elements $M_{14;41;44}(\lambda_2)$ it was shown in [1-4]:

$$\begin{cases} M_{14}(\lambda_2) = \varphi_{12} f_{24} + \varphi_{13} f_{34} + \phi_{14}\varphi_{44} f_{44} = \phi_{14}\varphi_{44} f_{44}, \\ M_{41}(\lambda_2) = \phi_{41}, \\ M_{44}(\lambda_2) = \phi_{41}\varphi_{12} f_{24} + \phi_{41}\varphi_{13} f_{34} + \varphi_{44} f_{44} = \varphi_{44} f_{44}. \end{cases} \quad (1)$$

Here:

f_{ik} - elements of the phase anisotropy matrix taking into account the "spectral" correction of the phase shift $\delta(\lambda_2) = \frac{\lambda_2}{\lambda_1}\delta(\lambda_1)$;

φ_{ik} - linear dichroism matrix elements $\varphi_{ik} = \begin{cases} \varphi_{12} = \varphi_{21} = (1-\Delta\tau)\cos 2\rho, \\ \varphi_{13} = \varphi_{31} = (1-\Delta\tau)\sin 2\rho, \\ \varphi_{22} = (1+\Delta\tau)\cos^2 2\rho + 2\sqrt{\Delta\tau}\sin^2 2\rho, \\ \varphi_{23} = \varphi_{32} = (1-\Delta\tau)\sin 2\rho, \\ \varphi_{33} = (1+\Delta\tau)\sin^2 2\rho + 2\sqrt{\Delta\tau}\cos^2 2\rho, \\ \varphi_{44} = 2\sqrt{\Delta\tau}. \end{cases}$, (2)

where $\Delta\tau = \frac{\tau_x}{\tau_y}$, $\begin{cases} \tau_x = \tau\cos\rho; \\ \tau_y = \tau\sin\rho \end{cases}$, τ_x, τ_y - absorption coefficients of linearly polarized orthogonal components of the amplitude of the laser radiation;

Advanced Topics in Optoelectronics, Microelectronics and Nanotechnologies X, edited by Marian Vladescu, Razvan Tamas, Ionica Cristea, Proc. of SPIE Vol. 11718, 117181J
 · doi: 10.1117/12.2571213

ϕ_{ik} - elements of the matrix of circular dichroism $\phi_{ik} = \begin{cases} \phi_{22} = \phi_{33} = \dfrac{1-\Delta g^2}{1+\Delta g^2}, \\ \phi_{14} = \phi_{41} = \pm\dfrac{2\Delta g}{1+\Delta g^2}. \end{cases}$, (3)

where $\Delta g = \dfrac{g_\otimes - g_\oplus}{g_\otimes + g_\oplus}$, $g_\otimes$, $g_\oplus$ - absorption coefficients of the right- ($\otimes$) and left- ($\oplus$) circularly polarized components of the amplitude of the laser radiation.

The solutions of the system of equations (1) - (3) are the following algorithms of the Mueller-matrix reconstruction of the parameters of linear and circular dichroism

$$\Delta\tau = 0{,}25\frac{M_{44}(\lambda_2)}{M_{44}(\lambda_1)} \times \frac{\lambda_2}{\lambda_1}, \tag{4}$$

$$\Delta g = 1 + \left(1 - M_{41}(\lambda_2)\right)^{0{,}5}. \tag{5}$$

2. Optical scheme of two-dimensional spectral-selective stockpolarimetry and its characteristics

Measurement of coordinate distributions (two-dimensional arrays of values in the sample plane) of the values of the elements of the Mueller matrices was performed in the location (Fig. 1) of a standard stockpolarimeter [5-9].

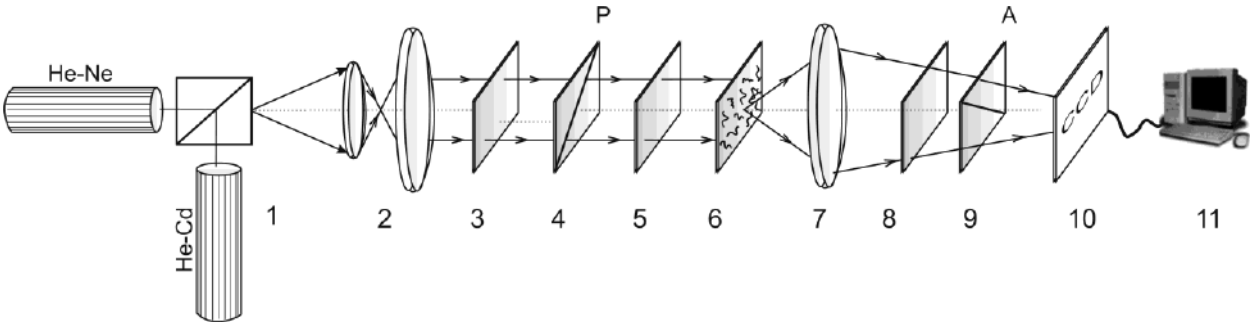

Fig. 1. Optical scheme of "two-wave" spectral-selective stockpolarimeter

Irradiation of samples 6 was sequentially performed by a parallel ($Ø = 2\times10^3\,\mu m$) beam of "red" He-Ne ($\lambda_1 = 0.6328\mu m$) and semiconductor "blue" ($\lambda_2 = 0.405\mu m$) lasers 1. The polarizing irradiator consisted of a quarter-wave plate 3 and a polarizer 4. Images of samples 6 using a polarizing microlens 7 (Nikon) CFI Achromat P, focal length - 30mm, aperture - 0.1, magnification - 4x) was projected into the plane of the light-sensitive plane of the CCD camera 10 (The Imaging Source DMK 41AU02.AS, monochrome 1/2 "CCD, Sony ICX205AL (progressive scan); ability - 1280x960, the size of the light-sensitive plane - 7600x6200 microns, sensitivity - 0.05 lx, dynamic range - 8 bit) Polarization analysis of images of samples 6 was performed using a quarter-wave plate 8 and a polarizer 9.

The calculation within each pixel of the digital camera 10 of the set of elements of the Mueller matrix of the sample 6 was performed in accordance with the algorithm [6, 8]

$$
\begin{aligned}
M_{11} &= 0.5(V_1^0 + V_1^{90}); & M_{21} &= 0.5(V_2^0 + V_2^{90});\\
M_{12} &= 0.5(V_1^0 - V_1^{90}); & M_{22} &= 0.5(V_2^0 - V_2^{90});\\
M_{13} &= V_1^{45} - M_{11}; & M_{23} &= V_2^{45} - M_{21};\\
M_{14} &= V_1^{\otimes} - M_{11}; & M_{24} &= V_2^{\otimes} - M_{21};\\
M_{31} &= 0.5(V_3^0 + V_3^{90}); & M_{41} &= 0.5(V_4^0 + V_4^{90});\\
M_{32} &= 0.5(V_3^0 - V_3^{90}); & M_{42} &= 0.5(V_4^0 - V_4^{90});\\
M_{33} &= V_3^{45} - M_{31}; & M_{43} &= V_4^{45} - M_{41};\\
M_{34} &= V_3^{\otimes} - M_{31}; & M_{44} &= V_4^{\otimes} - M_{41}.
\end{aligned}
\tag{6}
$$

Here $V_{i=2;3;4}^{0;45;90;\otimes}$ are the parameters of the Stokes vector of the points of the digital image of sample 6, measured for a series of linearly (0^0; 45^0; 90^0) and right-circular ($\otimes$) polarized laser beams

$$
\begin{aligned}
V_{i=1}^{0;45;90;\otimes} &= I_0^{0;45;90;\otimes} + I_{90}^{0;45;90;\otimes};\\
V_{i=2}^{0;45;90;\otimes} &= I_0^{0;45;90;\otimes} - I_{90}^{0;45;90;\otimes};\\
V_{i=3}^{0;45;90;\otimes} &= I_{45}^{0;45;90;\otimes} - I_{135}^{0;45;90;\otimes};\\
V_{i=4}^{0;45;90;\otimes} &= I_{\otimes}^{0;45;90;\otimes} + I_{\oplus}^{0;45;90;\otimes}.
\end{aligned}
\tag{7}
$$

Here - the intensity of light transmitted by an object passing through a linear polarizer 9 with the angle of rotation of the transmission plane 0^0; 45^0; 90^0; 135^0 :, as well as through the system "quarter-wave plate 8 - polarizer 9, which transmits right- ($\otimes$) and left- ($\oplus$) circularly polarized components object laser radiation.

3. Experimental results and their discussion

As the objects of study, we used optically thin (geometric thickness $d \approx 25\mu m \div 30\mu m$, attenuation coefficient τ p 0.1) histological sections of a biopsy of cervical tissue - endometrium in a precancerous state of two types:

- simple endometrial atrophy - group 1 (36 samples)
- endometrial polyp - group 2 (36 samples).

In the series of fig. 2 - fig. 3 shows the results of the Mueller-matrix reconstruction of the distribution of the values of the parameters of the amplitude ($\Delta\tau$) endometrial anisotropy with simple atrophy (fig. 1) and with a polyp (fig. 2-4). Each figure consists of coordinate (fragments (1), (2)) and topographic (fragments (3)) distributions of the coefficient of linear dichroism $\Delta\tau$. Topographic distributions are a system of lines of equal values $[\Delta\tau = 0{,}5](m \times n)$.

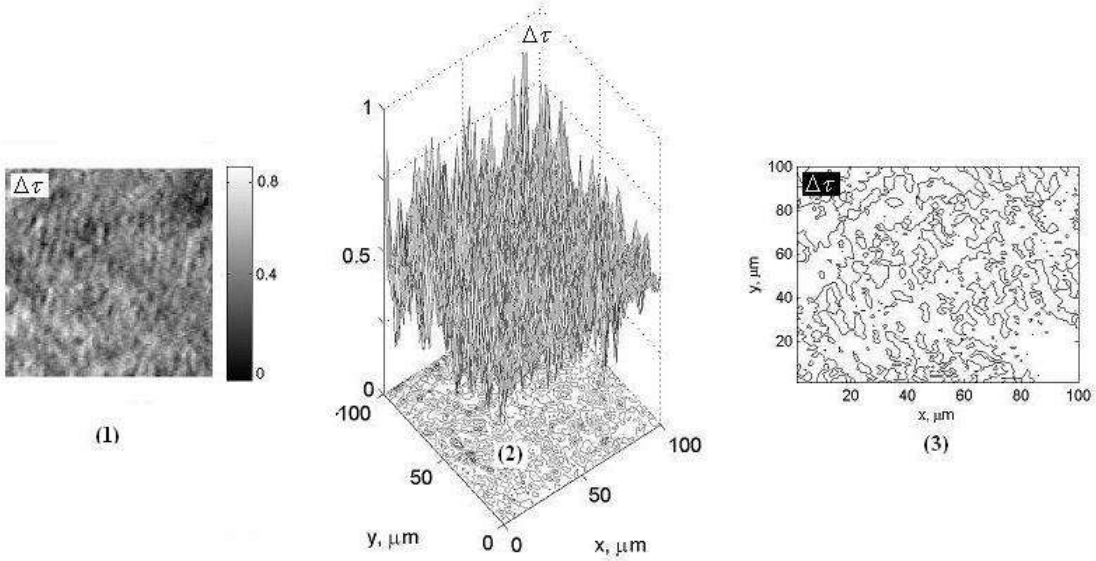

Fig. 2. Two-dimensional $2D-\Delta\tau(m\times n)$, three-dimensional $3D-\Delta\tau(m\times n)$ and topographic $[\Delta\tau=0,1\pi](m\times n)$ distributions of the values of the linear dichroism $\Delta\tau$ parameter of the histological section of an endometrial biopsy with simple atrophy.

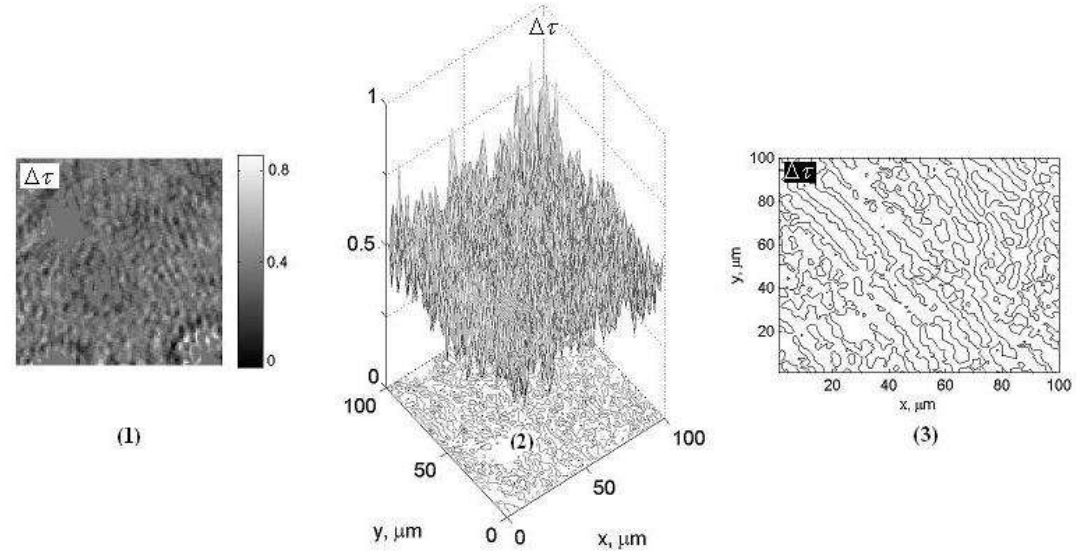

Fig. 3. Two-dimensional $2D-\Delta\tau(m\times n)$, three-dimensional $3D-\Delta\tau(m\times n)$ and topographic $[\Delta\tau=0,1\pi](m\times n)$ distributions of the values of the linear dichroism $\Delta\tau$ parameter of the histological section of an endometrial biopsy of the endometrial polyp.

A statistical analysis of the coordinate distributions of the values of the linear dichroism $\Delta\tau(m\times n)$ index of the endometrial layers in the precancerous state revealed a slightly larger range (up to 60% -70%) of the differences between the values $Z_{i=1;2;3;4}(\Delta\tau)$.

The following data on the linear dichroism of histological endometrial sections were obtained:

- with atrophy - $Z_1(\Delta\tau)=0,49,\quad Z_2(\Delta\tau)=0,24,\quad Z_3(\Delta\tau)=0,63,\quad Z_4(\Delta\tau)=0,84$;
- polyp - $Z_1(\Delta\tau)=0,52,\quad Z_2(\Delta\tau)=0,19,\quad Z_3(\Delta\tau)=0,91,\quad Z_4(\Delta\tau)=1,09$.

As can be seen, for the polyp biopsy sample, there is a decrease ($Z_2 \downarrow$) in the statistical moment of the 2nd order (1.26 times) and an increase in the magnitude of the statistical moments of the 3rd ($Z_3 \uparrow$ - 1.44 times) and 4th ($Z_4 \uparrow$ - 1.3 times) orders. This fact indicates the sensitivity (the range of differences between the statistical moments characterizing the distribution of the values of the anisotropy parameters) of the polarization reproduction of the linear dichroism parameter $\Delta\tau$.
The values of statistical moments averaged within both groups of samples are shown in table 1.

Table 1. Statistical moments of the 1st - 4th order characterizing the distribution of the values of the parameters of linear dichroism of histological sections of the endometrium

Z_i	$\Delta\tau$, $n_1 = n_2 = 36$	
	Atrophy	Polyp
Z_1	$0{,}48 \pm 0{,}037$	$0{,}53 \pm 0{,}041$
Z_2	$0{,}18 \pm 0{,}013$	$0{,}23 \pm 0{,}021$
Z_3	$0{,}69 \pm 0{,}058$	$0{,}95 \pm 0{,}089$
Z_4	$0{,}81 \pm 0{,}077$	$1{,}04 \pm 0{,}099$

Table 2. Balanced accuracy of the method of Mueller-matrix reconstruction of the polycrystalline structure of histological sections of the endometrial biopsy

Z_i	$Ac(\Delta\tau),\%$
Z_1	61,1
Z_2	63,9
Z_3	77,8
Z_4	77,8

Conclusions

This method is aimed at differentiating the manifestations of optical anisotropy of samples very close in morphological structure that are found in a precancerous state. Therefore, the achieved level of accuracy ($Ac(\Delta\tau) = 77{,}8\%$) in terms of evidence-based medicine corresponds to a good level.

References

[1]. R. Ossikovski, V. Devlaminck, " General criterion for the physical realizability of the differential Mueller matrix," Opt. Lett. 39, 1216-1219 (2014).
[2]. V. Devlaminck and R. Ossikovski, "Uniqueness of the differential Mueller matrix of uniform homogeneous media," Opt. Lett. 39, 3149-3152 (2014).
[3]. V. Devlaminck, "Physical model of differential Mueller matrix for depolarizing uniform media," J. Opt. Soc. Am. 30, 2196-2204 (2013) .
[4]. Ushenko, A.G., Dubolazov, O.V., Bachynsky, V.T., Peresunko, A.P., Vanchulyak, O.Y., "On the feasibilities of using the wavelet analysis of mueller matrix images of biological crystals," (2010) Advances in Optical Technologies, 162832.

[5]. Zabolotna, N.I., Wojcik, W., Pavlov, S.V., Ushenko, O.G., Suleimenov, B., "Diagnostics of pathologically changed birefringent networks by means of phase Mueller matrix tomography," (2013) Proceedings of SPIE - The International Society for Optical Engineering, 8698, 86980.
[6]. Ushenko, A.G., "Correlation Processing and Wavelet Analysis of Polarization Images of Biological Tissues," (2001) Optics and Spectroscopy (English translation of Optika i Spektroskopiya), 91 (5), pp. 773-778.
[7]. Ushenko, A.G., Ermolenko, S.B., Burkovets, D.N., Ushenko, Yu.A., "Polarization microstructure of laser radiation scattered by optically active biotissues," (1999) Optika i Spektroskopiya, 87 (3), pp. 470-474.
[8]. Ushenko, A.G., Dubolazov, A.V., Ushenko, V.A., Novakovskaya, O.Y., "Statistical analysis of polarization-inhomogeneous Fourier spectra of laser radiation scattered by human skin in the tasks of differentiation of benign and malignant formations," (2016) Journal of Biomedical Optics, 21 (7), 071110.
[9]. Bekshaev AY, Angelsky OV, Sviridova SV, Zenkova CY. Mechanical action of inhomogeneously polarized optical fields and detection of the internal energy flows. Adv Opt Technol 2011.
[10]. Angelsky, O. V., Maksimyak, P. P., &Perun, T. O. (1993). Optical correlation method for measuring spatial complexity in optical fields. Optics Letters, 18(2), 90-92.
[11]. Angelsky, O. V., Bekshaev, A. Y. A., Maksimyak, P. P., Maksimyak, A. P., & Hanson, S. G. (2018). Low-temperature laser-stimulated controllable generation of micro-bubbles in a water suspension of absorptive colloid particles. Optics Express, 26(11), 13995-14009.
[12]. Angelsky, O. V. (2007). Optical correlation techniques and applications. Optical correlation techniques and applications (pp. 1-270).
[13]. Angelsky, O. V., Ushenko, A. G., Pishak, V. P., Burkovets, D. N., Yermolenko, S. B., Pishak, O. V., &Ushenko, Y. A. (2000). Coherent introscopy of phase-inhomogeneous surfaces and layers. Paper presented at the Proceedings of SPIE - the International Society for Optical Engineering, 4016 413-418.